LES OF TURBULENCE MODULATION IN DIFFUSION FLAMES

Bernard J. Geurts
Multiscale Modeling and Simulation, J.M. Burgers Center,
Faculty EEMCS, University of Twente, P.O. Box 217,
7500 AE Enschede, The Netherlands
Anisotropic Turbulence, Fluid Dynamics Laboratory,
Department of Applied Physics, Eindhoven University of Technology, P.O. Box 513,
5300 MB Eindhoven, The Netherlands
b.j.geurts@utwente.nl

Rob J.M. Bastiaans
Combustion Technology, Department of Mechanical Engineering,
Eindhoven University of Technology, P.O. Box 513,
5300 MB Eindhoven, The Netherlands
r.j.m.bastiaans@tue.nl

ABSTRACT

We analyze the evolution of a diffusion flame in a turbulent mixing layer using large-eddy simulation. The large-eddy simulation includes Leray regularization of the convective transport and approximate inverse filtering to represent the chemical source terms. Attention is focused on the interaction between turbulence and combustion. The Leray model is compared to the more conventional dynamic mixed model, concentrating on the kinetic energy decay, the spectrum and the mixing rate.

INTRODUCTION

In various combustion processes turbulent diffusion flames arise. These are characterized by a thin, distorted and lively evolving region where the conditions for combustion, such as presence of chemical species at appropriate concentration and temperature, are fulfilled (Peters, 2000). We will consider combustion in a turbulent mixing layer with stylized chemical reaction process (Geurts, 2005). This computational model can be treated in full detail and provides an impression of the dominant turbulence modulation that arises from the coupling between the fluid-flow and the chemical reaction equations.

It is the purpose of this paper to analyze the capabilities of large-eddy simulation of diffusion flames. This requires a proper capturing of the three central closure problems, i.e., for *(i)* the turbulent stresses, *(ii)* the velocity-species correlations and *(iii)* the chemical source terms. We will focus on a comparison between Leray regularization (Geurts and Holm, 2003, 2006) and dynamic mixed modeling (Zang et al., 1993 and Vreman et al., 1994) for the turbulent stresses. These types of modeling may also be adopted to express the velocity-species correlations. In addition, we will consider an inverse modeling (Geurts, 1997, Kuerten et al. 1999) of the chemical source terms. Specifically, the filtered nonlinear source terms are formulated in 'reconstructed' flow variables. This requires the application of an approximate inversion of the spatial large-eddy filter.

Compared to the dynamic mixed modeling, the regularization modeling of the turbulent stresses will be shown to better retain the small-scale variability of a turbulent flow. To illustrate this, the mixing-rate and the kinetic energy spectrum are determined under combustion conditions. The regularization and dynamic mixed models properly capture the reduced mixing at high heat-release. The Leray model predicts a significantly higher tail of the kinetic energy spectrum compared to the dynamic mixed model. This also affects important global flame-properties such as the evolving surface-area and wrinkling of the flame.

DIFFUSION FLAME IN A MIXING LAYER

Mathematical model of simplified combustion

The computational model is composed of the compressible flow equations for ideal gases, coupled to a system of advection-diffusion-reaction equations (Pope, 2000, Geurts 2003). The dimensionless system of equations that is considered here can be expressed in three dimensions as

$$\partial_t \rho + \partial_j(\rho u_j) = 0 \qquad (1)$$

$$\partial_t(\rho u_i) + \partial_j(\rho u_i u_j) + \partial_i p - \partial_j \sigma_{ij} = 0 \qquad (2)$$

$$\partial_t e + \partial_j((e+p)u_j) - \partial_j(\sigma_{ij}u_i) + \partial_j q_j - h_k\omega_k = 0 \qquad (3)$$

$$\partial_t(\rho c_k) + \partial_j(\rho c_k u_j) - \partial_j(\pi_{kj}) - \omega_k = 0 \qquad (4)$$

where ρ denotes the fluid mass-density, u_i the velocity in the x_i direction, e the total energy density and c_k the k-th chemical species concentration. We consider N_s different species. Partial derivatives with respect to time t and spatial coordinate x_i are denoted by ∂_t and ∂_i respectively. Summation over repeated indices is implied. The continuity equation (1) represents conservation of mass. The conservation principles for momentum and energy are contained in (2) and (3). The latter equation contains in addition contributions from heat released by the chemical processes. Finally, the conservation principle for the individual species is provided in (4).

In order to close this system of equations, additional constitutive relations need to be provided. We follow the standard description given in Geurts (2003). The viscous fluxes are specified by $\pi_{kj} = \partial_j c_k/(Re\,Sc)$ and $\sigma_{ij}(\mathbf{u}) = S_{ij}/Re$, with rate of strain tensor given by

$$S_{ij} = \partial_i u_j + \partial_j u_i - \frac{2}{3}\delta_{ij}\partial_k u_k \qquad (5)$$

The Reynolds (Re) and Schmidt (Sc) numbers characterize the strength of the viscous fluxes relative to the nonlinear

convective contributions in the momentum and species equations. Throughout we will adopt $Sc = 10$. The equation of state for an ideal gas specifies the pressure p through

$$e = \frac{p}{\gamma - 1} + \frac{1}{2}\rho u_i u_i \tag{6}$$

where the adiabatic constant $\gamma \approx 7/5$. The heat flux vector is given by

$$q_j = -\frac{\partial_j T}{(\gamma - 1)RePrM^2} \tag{7}$$

where Pr is the Prandtl number, M the Mach number and the temperature T follows from the ideal gas law $\rho T = \gamma M^2 p$. Throughout we put $Pr = 1$ and $M = 0.2$. The chemical reactions associated with the combustion are described by source terms in the energy equation (3) and the species equations (4). We turn to this part of the computational model next.

A large class of chemical reactions may be expressed in terms of a multi-species, multi-step process (bastiaans et al., 2001). In general, the N_s chemical species may be involved in N_c chemical reactions. Let $\mathcal{M}_i$ denote the chemical species and $\nu^r_{i,l}$, $\nu^p_{i,l}$ the stoichiometric coefficients of the i-th species, viewed as reactants (r) and products (p) in the l-th reaction, respectively. The multi-species, multi-step chemical reaction involves transitions that may be expressed as:

$$\nu^r_{i,l}\mathcal{M}_i \rightarrow \nu^p_{i,l}\mathcal{M}_i \quad ; \quad l = 1, \ldots, N_c \tag{8}$$

This describes the l-th reaction in which $\nu^r_{i,l}$ 'units' of species $\mathcal{M}_i$, $i = 1, \ldots, N_s$ give rise to $\nu^p_{i,l}$ units after the reaction. We will consider only a single, very simple reaction in which a fuel F reacts with an oxidizer O to yield a product P:

$$F + O \rightarrow P \tag{9}$$

This particular combustion model involves $N_s = 3$ species in $N_c = 1$ reaction in which $\nu^r_F = \nu^r_O = 1$ units of fuel and oxidizer combine into $\nu^p_P = 1$ units of product. In this stylized description fuel and oxidizer are lost after the reaction, i.e., $\nu^p_F = \nu^p_O = 0$ while there was no product ahead of the reaction, i.e., $\nu^r_P = 0$. In the sequel we associate F with species 1, O with species 2 and P with species 3.

The chemical reaction rate ω_i is assumed to be determined by the Arrhenius law (Peters, 2000):

$$\frac{\omega_i}{W_i} = (\nu^p_{i,l} - \nu^r_{i,l})Da_l \exp(-\frac{Ze_l}{T}) \prod_{k=1}^{N_s} \left(\frac{\rho c_k}{W_k}\right)^{\nu^r_{k,l}} \tag{10}$$

where summation over l is implied and W_i is the molecular weight of species $\mathcal{M}_i$. Moreover, Da_l and Ze_l denote the Damköhler and Zeldovich numbers respectively of the l-th reaction. For the particular reaction $F + O \rightarrow P$ we can simplify the expressions for the reaction-rates further and obtain:

$$\omega_1 = -(\rho c_F)(\rho c_O)\frac{Da}{W_O}\exp(-\frac{Ze}{T}) \tag{11}$$

$$\omega_2 = -(\rho c_F)(\rho c_O)\frac{Da}{W_F}\exp(-\frac{Ze}{T}) \tag{12}$$

$$\omega_3 = (\rho c_F)(\rho c_O)\frac{DaW_P}{W_F W_O}\exp(-\frac{Ze}{T}) \tag{13}$$

Since $W_P = W_F + W_O$ we may write

$$\frac{DaW_P}{W_F W_O} = \frac{Da(W_F + W_O)}{W_F W_O} = Da_O(1 + \alpha) \tag{14}$$

where we introduced the 'compensated' Damköhler number $Da_O = Da/W_O$ and the weight-ratio $\alpha = W_O/W_F$. Correspondingly, we infer

$$\omega_2 = \alpha\omega_1 \quad ; \quad \omega_3 = -(1 + \alpha)\omega_1 \tag{15}$$

The source term in the energy equation can be expressed as

$$\begin{aligned} h_j\omega_j &= h_1\omega_1 + h_2\omega_2 + h_3\omega_3 \\ &= \omega_1(h_1 + \alpha h_2 - (1 + \alpha)h_3) = Q\omega_1 \end{aligned} \tag{16}$$

where the individual enthalpies are denoted by h_j and Q will be referred to as the effective standard enthalpy of formation. In total the combustion model requires the evaluation of ω_1 and four additional parameters: Da_O, Ze, Q and α. Throughout we will adopt $Da_O = 1$, $Ze = 1$ and $\alpha = 1$ and focus on effects arising from variations in Q. The validity of these parameter-values in real combustion processes needs to be investigated to improve the physical understanding of the observed phenomena. This requires an extensive parameter-study which is subject of ongoing research.

Numerical method for diffusion flame

We simulate the compressible three-dimensional temporal mixing layer and use a Reynolds number based on the upper stream velocity and half the initial vorticity thickness of 50 (Vreman et al., 1997). The governing equations are solved in a cubic geometry of side ℓ which is set equal to four times the wavelength of the most unstable mode according to linear stability theory, i.e., under the chosen conditions $\ell = 59$. Periodic boundary conditions are imposed in the streamwise (x_1) and spanwise (x_3) direction, while in the normal (x_2) direction the boundaries are free-slip walls. The initial condition is formed by mean profiles corresponding to constant pressure $p = 1/(\gamma M^2)$, $u_1 = \tanh(x_2)$ for the streamwise velocity component, $u_2 = u_3 = 0$ and a temperature profile given by the Busemann-Crocco law. Superimposed on the mean profile are two- and three-dimensional perturbation modes obtained from linear stability theory.

We use explicit time-integration with a second order, compact storage, four-stage Runge-Kutta scheme. A fourth order accurate spatial discretization method is adopted for the convective fluxes while a second order central finite volume scheme is used for the viscous fluxes.

Visualization of the flow under conditions studied here demonstrates the roll-up of the fundamental instability. Four rollers with mainly negative spanwise vorticity develop. These undergo two distinct pairings. After the first pairing the flow has become highly three-dimensional. Another pairing yields a single roller in which the flow exhibits a complex structure, with many regions of positive spanwise vorticity.

The consequences of combustion for turbulence dynamics may be investigated within the basic temporal mixing layer configuration. In this paper we consider initially the upper stream to contain fuel ($c_F = 1, c_O = 0$) and the lower stream to contain oxidizer ($c_O = 1, c_F = 0$). The initial condition is assumed to contain no 'product' ($c_P = 0$).

LARGE-EDDY MODELING OF DIFFUSION FLAMES

Spatial filtering and subgrid closure

In the filtering approach to large-eddy simulation, a spatial convolution filter is applied to the governing equations given by (1)-(4). Specifically, we introduce the filtered field

$\overline{f}$ associated with an unfiltered field f through

$$\overline{f}(\mathbf{x},t) = L(f) = \int_{-\infty}^{\infty} G(\mathbf{x}-\boldsymbol{\xi})u(\boldsymbol{\xi},t)\, d\boldsymbol{\xi} \qquad (17)$$

where the filter-kernel G has a width Δ and we assume $G(\mathbf{z}) = G_1(z_1)G_2(z_2)G_3(z_3)$, i.e., the product of three filter-kernels associated with filtering in the x_1, x_2 and x_3 directions respectively. We assume that the filter L is normalized. Next to this basic filter, it is convenient to define the corresponding Favre filter in which

$$\widetilde{f} = \frac{\overline{\rho f}}{\overline{\rho}} = \frac{L(\rho f)}{L(\rho)} = L_\rho(f) \qquad (18)$$

in terms of the Favre operator L_ρ.

Application of the spatial filter L to (1)-(4) results in the following system of equations:

$$\partial_t \overline{\rho} + \partial_j(\overline{\rho}\widetilde{u}_j) = 0 \qquad (19)$$

$$\partial_t(\overline{\rho}\widetilde{u}_i) + \partial_j(\overline{\rho}\widetilde{u}_i\widetilde{u}_j) + \partial_i\overline{p} - \partial_j\breve{\sigma}_{ij} = -\partial(\overline{\rho}\tau_{ij}) + \partial_j(\overline{\sigma}_{ij} - \breve{\sigma}_{ij}) \qquad (20)$$

$$\partial_t\breve{e} + \partial_j((\breve{e}+\overline{p})\widetilde{u}_j) - \partial_j(\breve{\sigma}_{ij}\widetilde{u}_i) + \partial_j\breve{q}_j = \mathcal{A} + \overline{h_k\omega_k} \qquad (21)$$

$$\partial_t(\overline{\rho}\widetilde{c}_k) + \partial_j(\overline{\rho}\widetilde{c}_k\widetilde{u}_j) - \partial_j(\breve{\pi}_{kj}) = -\partial_j(\overline{\rho}\zeta_{jk}) + \partial(\overline{\pi}_{kj} - \breve{\pi}_{kj}) + \overline{\omega}_k \qquad (22)$$

in terms of the filtered variables $\overline{\rho}$, $\widetilde{u}_j$, $\overline{p}$ and $\widetilde{c}_k$. In these equations we denote the smoothed viscous flux by $\breve{\sigma}_{ij} = \sigma_{ij}(\widetilde{\mathbf{u}})$ and obtain the smoothed energy and heat flux through

$$\breve{e} = \frac{\overline{p}}{(\gamma-1)} + \frac{1}{2}\widetilde{u}_i\widetilde{u}_i \qquad (23)$$

$$\breve{q}_j = -\frac{\partial_j\widetilde{T}}{(\gamma-1)RePrM^2} \qquad (24)$$

in which $\widetilde{T} = \gamma M^2\overline{p}/\overline{\rho}$. Moreover, the smoothed viscous fluxes in the species equations are given by $\breve{\pi}_{kj} = \partial_j\widetilde{c}_k/(ReSc)$. Apart from these contributions in terms of the filtered variables a number of additional contributions arises which constitute the combined closure problem. Filtering the energy equation gives rise to a large number of subgrid terms. These are summarized in the symbol $\mathcal{A}$. At low Mach number M the contributions of these closure terms can be neglected (Vreman et al., 1995). We restrict to such cases in the sequel, i.e., assume $\mathcal{A} \approx 0$. Terms such as $\overline{\sigma}_{ij} - \breve{\sigma}_{ij}$ and $\overline{\pi}_{kj} - \breve{\pi}_{kj}$ arise from the difference between the Favre (L_ρ) and the basic filter (L). In case compressibility effects are small these terms can be neglected. We will restrict to such conditions here. The filtered source terms $\overline{\omega}_k$ in (22) and the filtered heat-release term $\overline{h_k\omega_k}$ in (21) also need to be accounted for in the smoothed compressible equations. We discuss the modeling of these chemical source terms momentarily and next turn to the closure of the filtered convective terms, expressed by τ_{ij} and ζ_{jk}.

A variety of subgrid models has been proposed for the turbulent stress tensor and turbulent species fluxes, τ_{ij} and ζ_{jk}. In this paper we will compare dynamic mixed modeling (Vreman et al., 1994) with Leray regularization (Geurts and Holm, 2003). For notational convenience we present these models in their incompressible formulation. In actual simulations the compressible implementation is adopted.

The mixed model combines Bardina's similarity model (Bardina, 1984) with Smagorinsky's eddy-viscosity model (Smagorinsky, 1963). A dynamic version is derived on the basis of the application of Germano's identity (Germano et al., 1991, Germano, 1992) in which an explicit test filter is introduced. Then a least squares formulation for the coefficient according to Lilly (1992), is used, thereby assuming the coefficient to be a scalar. For further details we refer to Geurts (2003).

The mathematical regularization of the Navier-Stokes equations which we pursue here involves a direct and explicit alteration of the nonlinear convective terms. In the context of this paper, this provides a systematic framework for *deriving* a subgrid model which is in sharp contrast with traditional phenomenological subgrid modeling. Several basic regularization principles have been proposed, e.g., the NS-α model based on maintaining a filtered Kelvin circulation theorem (Geurts and Holm, 2003, 2006, Foias et al., 2001), or the Leray formulation (Leray, 1934) to which we will restrict in this paper.

In Leray regularization, one alters the convective fluxes into $\overline{u}_j\partial_j u_i$, i.e., the solution $\mathbf{u}$ is convected with a smoothed velocity $\overline{\mathbf{u}}$. Consequently, the nonlinear effects are reduced by an amount governed by the smoothing properties of the filter operation, L. The governing Leray equations are (Leray, 1934)

$$\partial_j\overline{u}_j = 0 \;\;;\;\; \partial_t u_i + \overline{u}_j\partial_j u_i + \partial_i p - \frac{1}{Re}\Delta u_i = 0 \qquad (25)$$

Leray solutions possess global existence and uniqueness with proper smoothness and boundedness, whose demonstration depends on the balance equation for $\int|\mathbf{u}|^2\, d^3x$. Based on the Leray equations (25) we may eliminate $\mathbf{u}$ by assuming $\overline{\mathbf{u}} = L(\mathbf{u})$ and $\mathbf{u} = L^{-1}(\overline{\mathbf{u}})$. For convolution filters one has, e.g., $\partial_t u_i = \partial_t(L^{-1}(\overline{u}_i)) = L^{-1}(\partial_t\overline{u}_i)$ and the nonlinear terms can be written as $\overline{u}_j\partial_j(u_i) = \partial_j(\overline{u}_j u_i) = \partial_j(\overline{u}_j L^{-1}(\overline{u}_i))$. Consequently, one may readily obtain:

$$L^{-1}\Big(\partial_t\overline{u}_i + \partial_j(\overline{u}_j\overline{u}_i) + \partial_i\overline{p} - \frac{1}{Re}\Delta\overline{u}_i\Big) = -\partial_j\Big(\overline{u}_j L^{-1}(\overline{u}_i) - L^{-1}(\overline{u}_j\overline{u}_i)\Big) \qquad (26)$$

This may be recast in terms of the LES template as:

$$\partial_t\overline{u}_i + \partial_j(\overline{u}_j\overline{u}_i) + \partial_i\overline{p} - \frac{1}{Re}\Delta\overline{u}_i = -\partial_j\Big(m_{ij}^L\Big) \qquad (27)$$

The implied asymmetric Leray model m_{ij}^L involves both L and its inverse and may be expressed as:

$$m_{ij}^L = L\Big(\overline{u}_j L^{-1}(\overline{u}_i)\Big) - \overline{u}_j\overline{u}_i = \overline{\overline{u}_j u_i} - \overline{u}_j\overline{u}_i \qquad (28)$$

The reconstructed solution u_i can in principle be found from any formal or approximate inversion L^{-1}. For this purpose one may use a number of methods, e.g., polynomial inversion (Geurts, 1997), geometric series expansions (Stolz and Adams, 1999) or exact numerical inversion of Simpson top-hat filtering (Kuerten et al., 1999) to which we return momentarily.

Similar to the turbulent stress tensor, the velocity-species stress tensor requires a closure model. Typically an eddy-diffusivity type formulation is adopted in literature in which $\zeta_{kj} \sim \partial_j\overline{c}_k$. Alternatively, the Leray regularization can be adopted also for ζ_{kj} leading to

$$\zeta_{kj} = L\Big(\overline{u}_j L^{-1}(\overline{c}_k)\Big) - \overline{u}_j\overline{c}_k = \overline{\overline{u}_j c_k} - \overline{u}_j\overline{c}_k \qquad (29)$$

An extension to compressible flow is quite straightforward and will not be described further here. Rather, we turn to

the filter inversion that is required for the Leray model. We will also adopt this to determine an explicit closure model for the chemical source terms.

Filter inversion and source-term modeling

The source term in the combustion model depends nonlinearly on the state-vector. Various models can be proposed for the source-term in the large-eddy context. Here, we will compare a model in terms of the filtered state vector with a model in which a partial inversion of the filter is adopted. For simplicity we focus on the stylized chemical reaction $F + O \rightarrow P$ introduced in the previous section. In this case only three species occur in a single chemical reaction and effectively only the filtered chemical source term $\overline{\omega}_1$ needs to be explicitly approximated. Once this source term is available we have $\overline{\omega}_2 = \alpha\overline{\omega}_1$, $\overline{\omega}_3 = -(1+\alpha)\overline{\omega}_1$ and $\overline{h_k\omega_k} = Q\overline{\omega}_1$.

The first model for the filtered source term uses an approximation in terms of the filtered state-vector:

$$\begin{aligned}\overline{\omega}_1 &= -Da_O\overline{(\rho c_F)(\rho c_O)\exp(-\frac{Ze}{T})} \\ &\approx -Da_O(\widetilde{\rho c_F})(\widetilde{\rho c_O})\exp(-\frac{Ze}{\widetilde{T}}) \end{aligned} \quad (30)$$

This model can be expected to capture the main dynamic contributions in cases where the filter-width Δ is quite small. Although this may not be the most challenging test for a large-eddy modeling, it does constitute a valuable point of reference.

The second model for $\overline{\omega}_1$ arises by invoking an approximation of the inversion of the spatial filter. In this case we arrive at a computational modeling in which

$$\overline{\omega}_1 \approx -Da_O\overline{(\rho^* c_F^+)(\rho^* c_O^+)\exp(-\frac{Ze}{T^+})} \quad (31)$$

Here $\rho^* = L^{-1}(\overline{\rho})$ and $f^+ = L_\rho^{-1}(\widetilde{f})$ in which L_ρ^{-1} denotes the approximate inverse of the Favre filter associated with L. The latter operator is applied to reconstruct some of the fine-scale structure in c_F, c_O and the temperature T. The evaluation of L_ρ^{-1} can readily be expressed in terms of L^{-1}. In fact, by definition of the Favre filter we have $L(\rho f) = L(\rho)L_\rho(f)$. Application of L^{-1} to this definition yields

$$L^{-1}\Big(L(\rho f)\Big) = \rho f = L^{-1}\Big(\overline{\rho}\widetilde{f}\Big) \quad (32)$$

From this relation we may isolate the unfiltered field f as

$$f = \frac{\rho f}{\rho} = \frac{L^{-1}\Big(\overline{\rho}\widetilde{f}\Big)}{L^{-1}(\overline{\rho})} \equiv L_\rho^{-1}(\widetilde{f}) \quad (33)$$

which defines the inversion of the Favre filter. Given $\widetilde{f}$ and $\overline{\rho}$ the inversion L_ρ^{-1} can be directly computed, provided the approximate inverse L^{-1} is available. The inversion L_ρ^{-1} can be applied to determine c_F^+, c_O^+ and T^+ that are required in this second model for $\overline{\omega}_1$.

There are various inversion procedures that may be adopted to approximate the inverse L^{-1}. A procedure that may be applied to general graded filters such as the top-hat or Gaussian filters arises from an expansion of L^{-1} in terms of a geometric series (Stolz and Adams, 1999):

$$\begin{aligned} L^{-1}(\overline{f}) &= \Big(I-(I-L)\Big)^{-1}(\overline{f}) = \sum_{n=0}^{\infty}(I-L)^n(\overline{f}) \\ &\approx \sum_{n=0}^{N}(I-L)^n(\overline{f}) \equiv L_N^{-1}(\overline{f}) \end{aligned} \quad (34)$$

Approximating the geometric series with $N+1$ terms we find the following computational inversion procedures:

$$\begin{aligned} N=0: \quad u^* &= L_0^{-1}(\overline{u}) = \overline{u} \\ N=1: \quad u^* &= L_1^{-1}(\overline{u}) = \overline{u} + (I-L)\overline{u} = 2\overline{u} - \overline{\overline{u}} \\ N=2: \quad u^* &= L_2^{-1}(\overline{u}) \\ &= \overline{u} + (I-L)\overline{u} + (I-L)(I-L)\overline{u} \\ &= 3\overline{u} - 3\overline{\overline{u}} + \overline{\overline{\overline{u}}} \end{aligned} \quad (35)$$

This method of approximate filter-inversion requires several applications of L, particularly in case of higher order inversion. Convergence toward the exact inverse is fastest in case the Fourier-transform of the filter-kernel is nowhere close to 0.

An alternative inversion procedure arises from the exact inversion of a particular numerical filter (Kuerten et al., 1999). In one dimension numerical convolution filtering corresponds to kernels

$$G(z) = \sum a_j\delta(z-z_j) \;\; ; \;\; |z_j| \leq \Delta/2 \quad (36)$$

In particular, we consider three-point filters with $a_0 = 1-\alpha$, $a_1 = a_{-1} = \alpha/2$ and $z_0 = 0$, $z_1 = -z_{-1} = \Delta/2$. Here we use $\alpha = 1/3$ which corresponds to Simpson quadrature of the top-hat filter. In actual simulations the resolved fields are known only on a set of grid points $\{x_m\}_{m=0}^N$. The application of L^{-1} to a general discrete solution $\{\overline{u}(x_m)\}$ can be specified using discrete Fourier transformation as in Kuerten et al. (1999),

$$L^{-1}(\overline{u}_m) = \sum_{j=-n}^{n}\left(\frac{\alpha-1+\sqrt{1-2\alpha}}{\alpha}\right)^{|j|}\frac{\overline{u}_{m+rj/2}}{(1-2\alpha)^{1/2}} \quad (37)$$

where the subgrid resolution $r = \Delta/h$ is assumed to be even. An accurate and efficient inversion can be obtained with only a few terms, recovering the original signal to within machine accuracy with $n \approx 10$. The sensitivity of the results to the inversion-accuracy was investigated and found not to be very critical.

The large-eddy simulations have been started from a suitably filtered initial condition as follows. In a first step a 256^3 representation of an initial condition for direct numerical simulations was generated. To obtain an initial condition for the large-eddy simulations, this field was filtered using the three-point Simpson quadrature approximation to the top-hat filter. The filter-width Δ was chosen identical to the filter-width that was selected for the subsequent large-eddy simulation. Throughout, we will adopt $\Delta = \ell/16$ (Geurts and Holm, 2006). In a second step the filtered data were restricted to the numerical grid of step-size Δx employed in the large-eddy simulations. Typical resolutions of 32^3, 64^3 and 96^3 were used, thereby covering the filter-width Δ by 2, 4 or 6 grid-cells respectively (Geurts and Fröhlich, 2002).

In the following section we investigate to what extent the closures of the turbulent stress tensor and the approximate closure of the chemical source terms contribute to accurate large-eddy simulation of diffusion flames. Specifically, alterations in the properties of the developing turbulent flow are assessed.

COMBUSTION-MODULATED TURBULENCE

In this section we investigate three central flow-properties associated with the combustion process in a transitional and turbulent temporal mixing layer. We will consider the decay of the resolved kinetic energy E, the growth of the momentum-thickness δ and the spectral distribution

of the energy $\mathcal{E}(k)$ in the turbulent regime. Specifically, The evolution of E illustrates the transitional flow and subsequent self-similar decay in the turbulent regime. It depends primarily on the larger scales in the flow. Similarly, the momentum thickness is a large-scale quantity that can be used as a measure for the progress of the mixing while the kinetic energy spectrum characterizes the prediction of both the large and the small scales in the flow. We focus on the influence of the heat-release parameter Q on the turbulent flow.

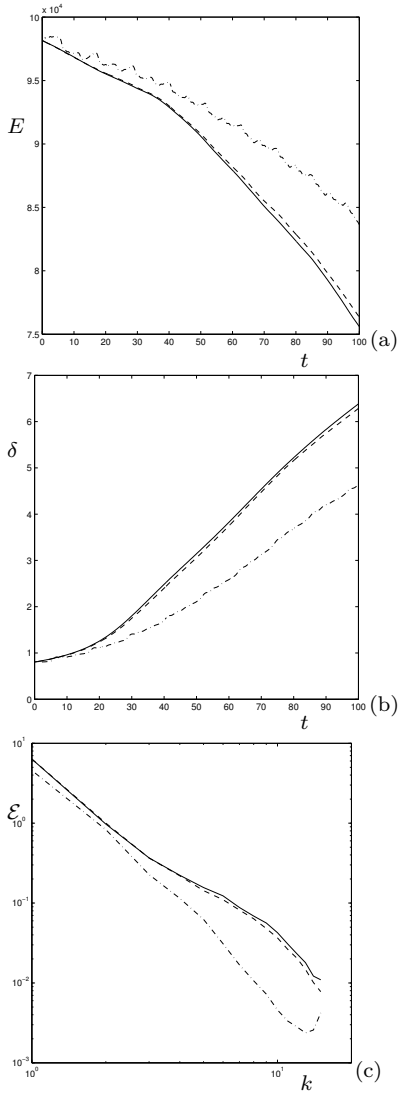

Figure 1: Decay of kinetic energy E (a), growth of momentum thickness δ (b) and kinetic energy spectrum $\mathcal{E}$ at a characteristic turbulent stage $t = 100$ (c). The resolution is 32^3 at $\Delta = \ell/16$ displaying the effect of the heat-release at $Q = -1$ (solid), $Q = -10$ (dashed), $Q = -100$ (dash-dotted).

In figure 1 we collected predictions obtained with the Leray regularization model for the turbulent stresses and inverse modeling of the chemical source terms. We observe a close similarity between predictions at $Q = -1$ and $Q = -10$, while a value $Q = -100$ leads to significant alterations compared to the no-combustion case. The decay of the kinetic energy is considerably reduced as the heat-release of the chemical process is increased (Fig. 1(a)). Moreover, a characteristic non-monotonous decay arises. We observe a strongly reduced mixing-rate at $Q = -100$ (Fig. 1(b)), as also reported in (bastiaans et al., 2001). This illustrates a remarkable competition in which the combustion process that actually requires mixing of fuel and oxidizer itself restricts this mixing. The effect is particularly strong for the small scales, as is clarified by the kinetic energy spectrum in the turbulent regime (Fig. 1(c)). The intense heat-release decreases the importance of the small scales which affects flame-wrinkling.

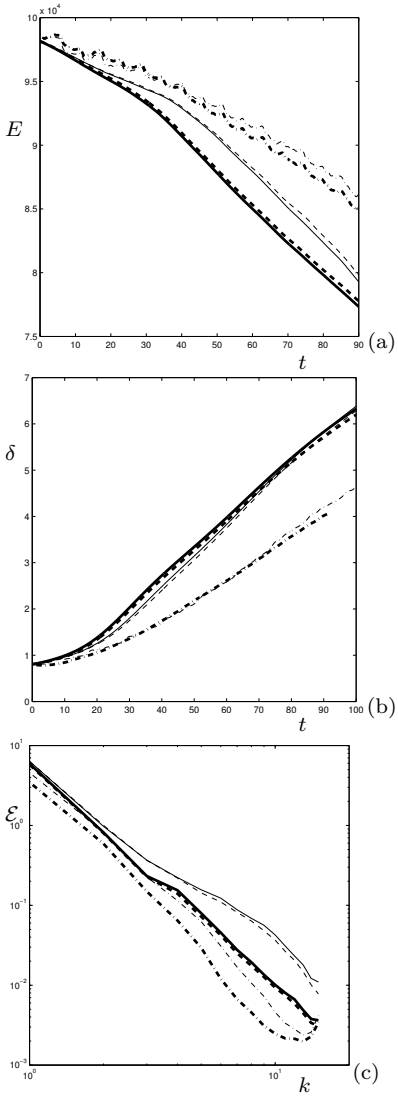

Figure 2: Comparison of Leray (thin lines) and dynamic mixed model (thick lines) predictions. Decay of kinetic energy E (a), growth of momentum thickness δ (b) and kinetic energy spectrum $\mathcal{E}$ at a characteristic turbulent stage $t = 100$ (c). The resolution is 32^3 at $\Delta = \ell/16$ displaying the effect of the heat-release at $Q = -1$ (solid), $Q = -10$ (dashed), $Q = -100$ (dash-dotted).

The results obtained by using the dynamic mixed subgrid model are compared with the Leray results in figure 2. We observe that the decay of the kinetic energy is more pronounced when use is made of the dynamic mixed model. This difference has hardly any influence on the prediction of the momentum thickness, while the small scales in the large-eddy solution are strongly reduced in case the dynamic mixed model is adopted. These differences in the large-eddy predictions affect the prediction of properties of the combus-

tion process. The use of inverse modeling for the chemical source terms was found to yield modest effects compared to the 'mean-model', at the parameters considered.

CONCLUDING REMARKS

In this paper, we introduced a simple combustion model and studied a turbulent diffusion flame in a temporal mixing layer. The coupling between the combustion and the turbulent transport induces a significant modulation of the turbulent flow properties, e.g., characterized by a strongly reduced spreading rate of the mixing layer. The dynamic mixed model was compared to the Leray regularization model for the turbulent stress tensor in large-eddy simulation. Moreover, a mean-flow parameterization of the filtered chemical source terms was confronted with a formulation based on approximate inversion. At the combustion - and flow-conditions studied here, the dependence of the predictions on the source-term modeling is quite limited. Likewise, the influence of the subgrid model is not very pronounced, which is all the more remarkable in view of the differences between these models and the fact that a coarse-grid simulation without any subgrid model yields significant differences. Evidently, the dynamic effects of the small scales in the flow are quite important and also well represented by either of the subgrid models.

The findings of this paper indicate that large-eddy simulation based on either the Leray or the dynamic mixed subgrid models yields qualitatively similar results. The Leray model appears to retain more of the small-scale variability in the flow which influences quantitatively a number of flow and combustion characteristics. The dynamic mixed subgrid model was found to be among the more accurate models describing turbulent mixing (Vreman et al., 1997). Here we find largely comparable results based on the Leray model (see also Geurts and Holm (2006)). However, compared to the intuitive modeling of the dynamic mixed model, the regularization principle that underlies the Leray formulation is much more transparent from a physics point of view. This is a main advantage that arises by starting from 'first principles' and is essential in case extension toward more complex situations is concerned. The regularization modeling that arises from the Lagrangian averaged Navier-Stokes framework (Foias et al., 2001) was found to be more accurate than the Leray model for turbulent mixing without combustion. Its extension to flows with combustion is subject of ongoing research and will be published elsewhere.

REFERENCES

Bardina, J., Ferziger, J.H., Reynolds, W.C., 1984, "Improved turbulence models based on LES of homogeneous incompressible turbulent flows", Department of Mechanical Engineering. *Report No. TF-19*, Stanford.

Bastiaans, R.J.M., Somers, L.M.T., de Lange, H.C., 2001, "DNS of non-premixed combustion in a compressible mixing layer", In: Modern strategies for turbulent flow simulation. Ed.: B.J. Geurts, R.T. Edwards Publishers, Philadelphia.

Foias, C., Holm, D.D., Titi, E.S., 2001, "The Navier-Stokes-alpha model of fluid turbulence", *Physica D*, **152**, 505.

Germano, M., Piomelli U., Moin P., Cabot W.H., 1991, "A dynamic subgrid-scale eddy viscosity model", *Phys.of Fluids*, **3**, 1760.

Germano, M., 1992, "Turbulence: the filtering approach", *J. Fluid Mech.*, **238**, 325.

Geurts, B.J., 1997, "Inverse Modeling for Large-Eddy Simulation", *Phys. of Fluids* **9**, 3585

Geurts B.J., 2003, "Elements of Direct and Large-Eddy Simulation", Edwards Publishing. ISBN: 1-930217-07-2.

Geurts, B.J., 2005, "Iso-surface analysis of a turbulent diffusion flame", *Proceedings ECMI-2004*, Springer Verlag, 222-228, ISBN: 3-540-28072-3

Geurts, B.J., Fröhlich, J., 2002, "A framework for predicting accuracy limitations in large-eddy simulation", *Phys. of fluids*, **14**, L41.

Geurts, B.J., Holm, D.D., 2003, "Regularization modeling for large-eddy simulation", *Phys. of Fluids*, **15**, L13

Geurts, B.J., Holm, D.D., 2006, "Leray and NS-α modeling of turbulent mixing", *J. of Turbulence*, **7** (10), 1 - 33.

Kuerten, J.G.M., Geurts, B.J., Vreman, A.W., Germano, M., 1999, "Dynamic inverse modeling and its testing in large-eddy simulations of the mixing layer", *Phys. of Fluids* **11**, 3778-3785

Leray, J., 1934, "Sur les movements d'un fluide visqueux remplaissant l'espace", *Acta Mathematica*, **63**, 193.

Lilly, D.K., 1992, "A proposed modification of the Germano subgrid-scale closure method", *Phys. of Fluids A*, **4**, 633.

Peters, N., 2000, "Turbulent combustion", Cambridge University Press. Cambridge, UK.

Pope, S.B., 2000, "Turbulent Flows", Cambridge University Press. Cambridge.

Smagorinsky, J., 1963, "General circulation experiments with the primitive equations", *Mon. Weather Rev.*, **91**, 99.

Stolz, S., Adams, N.A., 1999, "An approximate deconvolution procedure for large-eddy simulation", *Phys. of Fluids*, **11**, 1699.

Vreman, A.W., Geurts, B.J., Kuerten, J.G.M., 1994, "On the formulation of the dynamic mixed subgrid-scale model", *Phys. of Fluids* **6**, 4057

Vreman, A.W., Geurts, B.J., Kuerten, J.G.M., 1995, "Subgrid-modeling in LES of compressible flow", *Applied Scientific Research*, **54**, 191.

Vreman, A.W., Geurts, B.J., Kuerten, J.G.M., 1997, "Large-eddy simulation of the turbulent mixing layer", *J. Fluid Mech.*, **339**, 357.

Zang, Y., Street, R.L., Koseff, J.R., 1993, "A dynamic mixed subgrid-scale model and its application to turbulent recirculating flows", *Phys. of Fluids A*, **5**, 3186.